

An Improved Bound on the Optimal Paper Moebius Band

Richard Evan Schwartz ^{*}

December 15, 2020

Abstract

We show that a smooth embedded paper Moebius band must have aspect ratio at least

$$\lambda_1 = \frac{2\sqrt{4 - 2\sqrt{3}} + 4}{\sqrt[4]{3}\sqrt{2} + 2\sqrt{2\sqrt{3} - 3}} = 1.69497\dots$$

This bound comes more than 3/4 of the way from the old known bound of $\pi/2 = 1.5708\dots$ to the conjectured bound of $\sqrt{3} = 1.732\dots$

1 Introduction

This paper addresses the following question. *What is the aspect ratio of the shortest smooth paper Moebius band?* Let's state the basic question more precisely. Given $\lambda > 0$, let

$$M_\lambda = ([0, 1] \times [0, \lambda]) / \sim, \quad (x, 0) \sim (1 - x, \lambda) \quad (1)$$

denote the standard flat Moebius band of width 1 and height λ . This Moebius band has aspect ratio λ . Let $S \subset \mathbf{R}_+$ denote the set of values of λ such that

^{*}Supported by N.S.F. Grant DMS-1807320

there is a smooth¹ isometric embedding $I : M_\lambda \rightarrow \mathbf{R}^3$. The question above asks for the quantity

$$\lambda_0 = \inf S. \quad (2)$$

The best known result, due to Halpern and Weaver [HW], is that

$$\lambda_0 \in [\pi/2, \sqrt{3}]. \quad (3)$$

In §14 of their book, *Mathematical Omnibus* [FT], Fuchs and Tabachnikov give a beautiful exposition of the problems and these bounds. This is where I learned about the problem.

The lower bound is local in nature and does not see the difference between immersions and embeddings. Indeed, in [FT], a sequence of immersed examples whose aspect ratio tends to $\pi/2$ is given. The upper bound comes from an explicit construction. The left side of Figure 1.1 shows $M_{\sqrt{3}}$, together with a certain union of *bends* drawn on it. The right side shows the nearly embedded paper Moebius band one gets by folding this paper model up according to the bending lines.

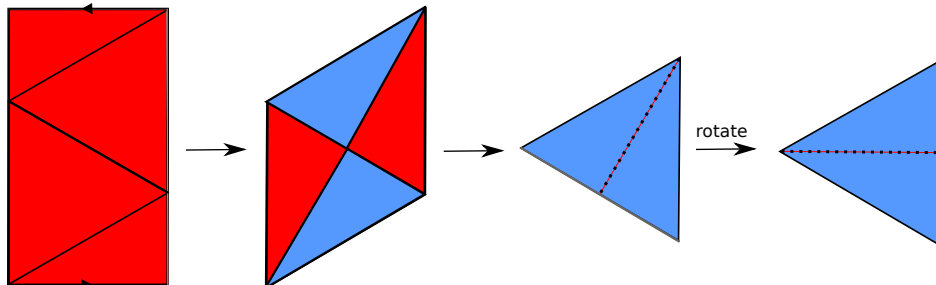


Figure 1.1: The conjectured optimal paper Moebius band

The Moebius band just described is degenerate: It coincides as a set with the equilateral triangle Δ of semi-perimeter $\sqrt{3}$. However, one can choose any $\epsilon > 0$ and find a nearby smoothly embedded image of $M_{\sqrt{3}+\epsilon}$ by a process of rounding out the folds and slightly separating the sheets. Halpern and

¹The smoothness requirement (or some suitable variant) is necessary in order to have a nontrivial problem. Given any $\epsilon > 0$, one can start with the strip $[0, 1] \times [0, \epsilon]$ and first fold it (across vertical folds) so that it becomes, say, an $(\epsilon/100) \times \epsilon$ “accordion”. One can then easily twist this “accordion” once around in space so that it makes a Moebius band. The corresponding map from M_ϵ is an isometry but it cannot be approximated by smooth isometric embeddings.

Weaver conjecture that $\lambda_0 = \sqrt{3}$, so that the triangular example is the best one can do.

The Moebius band question in a sense goes back a long time, and it is related to many topics. The early paper [Sa] proves rigorously that smooth paper Moebius bands exist. (See [HF] for a modern translation to english.) The paper [CF] gives a general framework for considering the differential geometry of developable surfaces. Some authors have discussed optimal shapes for Moebius bands from other perspectives, e.g. algebraic or physical. See, e.g. [MK] and [S1]. The Moebius band question has connections to origami. See e.g. the beautiful examples of isometrically embedded flat tori [AHLM]. It is also related to the main optimization question from geometric knot theory: What is the shortest piece rope one can use to tie a given knot? See e.g. [CKS].

In this paper we improve the lower bound. Because we do not want to worry about possible pathologies, we assume explicitly that the smooth extension of our map I to a neighborhood of M_λ is regular in the sense that the differential dI is 1-to-1 everywhere. This regularity will help us when we make polygonal approximations. We don't want to worry about any funny behavior at the boundary of M_λ .

Theorem 1.1 (Main) *An embedded paper Moebius band must have aspect ratio at least*

$$\lambda_1 = \frac{2\sqrt{4 - 2\sqrt{3}} + 4}{\sqrt[4]{3\sqrt{2} + 2\sqrt{2\sqrt{3} - 3}}} = 1.69497\dots$$

This value λ_1 arises naturally in a geometric optimization problem involving trapezoids. To quantify the way that our result improves over the previous lower bound, we note that $\lambda_1 > \sqrt{3} - (1/26)$ whereas $\pi/2 < \sqrt{3} - (4/26)$.

The proof of the Main Theorem has 2 ideas, which we now explain. Being a ruled surface, $I(M_\lambda)$ contains a continuous family of line segments which have their endpoints on $\partial I(M_\lambda)$. We call these line segments *bend images*. Say that a *T-pattern* is a pair of perpendicular coplanar bend images. The *T-pattern* looks somewhat like the two vertical and horizontal segments on the right side of Figure 1.1 except that the two segments are disjoint in an embedded example. Here is our first idea.

Lemma 1.2 *An embedded paper Moebius band of aspect ratio less than $7\pi/12$ contains a T-pattern.*

Note that $7\pi/12 > \sqrt{3}$, so Lemma 1.2 applies to the examples of interest to us. Lemma 1.2 relies crucially on the embedding property. The immersed examples in [FT] do not have these T -patterns.

The two bend images comprising the T -pattern divide $I(M)$ into two halves. Our second idea is to observe that the image $I(\partial M_\lambda)$ makes a loop which hits all the vertices of the T -pattern. When we compare the relevant portions of ∂M_λ with a polygon made from the vertices of the T -pattern, we get two constraints which lead naturally to the lower bound of λ_1 .

Since we can almost effortlessly give *some* improvement to the lower bound using Lemma 1.2, we do this now. The convex hull of the T -pattern contains a triangle of base at least 1 and height at least 1. Such a triangle has semi-perimeter at least $\phi = 1.61\dots$, the golden ratio. Hence $\lambda_0 \geq \phi$. The argument which gives $\lambda_0 \geq \lambda_1$, the constant in Theorem 1.1, is similar in spirit but more elaborate.

It would have been nice if the existence of a T -pattern forced $\lambda > \sqrt{3}$ on its own. This is not the case. In Figure 2.1 we show half of an immersed paper Moebius band of aspect ratio less than $\sqrt{3}$ that has a T -pattern. I did not try to formally prove that these exist, but using my computer program I can construct them easily. In a sequel paper I explain how to reduce the main conjecture above to some finite dimensional calculations (which currently are too hard for me to perform.)

This paper is organized as follows. In §2 we introduce polygonal paper Moebius bands and some basic geometric objects associated to them. We then prove Lemma 1.2 for polygonal Moebius bands. In §3 we give the argument involving the vertices of the T -pattern and thereby prove Theorem 1.1 for polygonal paper Moebius bands. In the brief §4 we explain why the results in the polygonal case imply the same results in the smooth case.

I would like to thank Dan Cristofaro-Gardiner, Dmitry Fuchs, Steve Miller, and Sergei Tabachnikov for helpful discussions about this problem. I would especially like to thank Sergei for telling me about the problem and pointing me to his book with Dmitry. I would also like to acknowledge the support of the Simons Foundation, in the form of a 2020-21 Simons Sabbatical Fellowship, and also the support of the Institute for Advanced Study, in the form of a 2020-21 membership funded by a grant from the Ambrose Monell Foundation.

2 Existence of the T Pattern

2.1 Polygonal Moebius Bands

Basic Definition: Say that a *polygonal Moebius band* is a pair $\mathcal{M} = (\lambda, I)$ where $I : M_\lambda \rightarrow \mathbf{R}^3$ is a map which is an isometry on each triangle. We insist that the vertices of these triangles all lie on ∂M_λ , as in Figure 1.1. In this paper we will work entirely with polygonal Moebius bands.

At the end of the paper, we will include a short chapter which explains why the results in the polygonal case imply the results in the smooth case.

Associated Objects: Let $\delta_1, \dots, \delta_n$ be the successive triangles of \mathcal{M} .

- The *ridge* of δ_i is edge of δ_i that is contained in ∂M_λ .
- The *apex* of δ_i to be the vertex of δ_i opposite the ridge.
- A *bend* is a line segment of δ_i connecting the apex to a ridge point.
- A *bend image* is the image of a bend under I .
- A *facet* is the image of some δ_i under I .

We always represent M_λ as a parallelogram with top and bottom sides identified. We do this by cutting M_λ open at a bend. See Figure 2.1 below.

The Sign Sequence: Let $\delta_1, \dots, \delta_n$ be the triangles of the triangulation associated to \mathcal{M} , going from bottom to top in P_λ . We define $\mu_i = -1$ if δ_i has its ridge on the left edge of P_λ and $+1$ if the ridge is on the right. The sequence for the example in Figure 1.1 is $+1, -1, +1, -1$.

The Core Curve: There is a circle γ in M_λ which stays parallel to the boundary and exactly $1/2$ units away. In Equation 1, this circle is the image of $\{1/2\} \times [0, \lambda]$ under the quotient map. We call $I(\gamma)$ the *core curve*.

The left side of Figure 2.1 shows M_λ and the pattern of bends. The vertical white segment is the bottom half of γ . The right side of Figure 2.1 (which has been magnified to show it better) shows $I(\tau)$ where τ is the colored half of M_λ . All bend angles are π and the whole picture is planar. The colored curve on the right is the corresponding half of the core curve. Incidentally, for τ we have $L + R = 1.72121\dots < \sqrt{3}$.

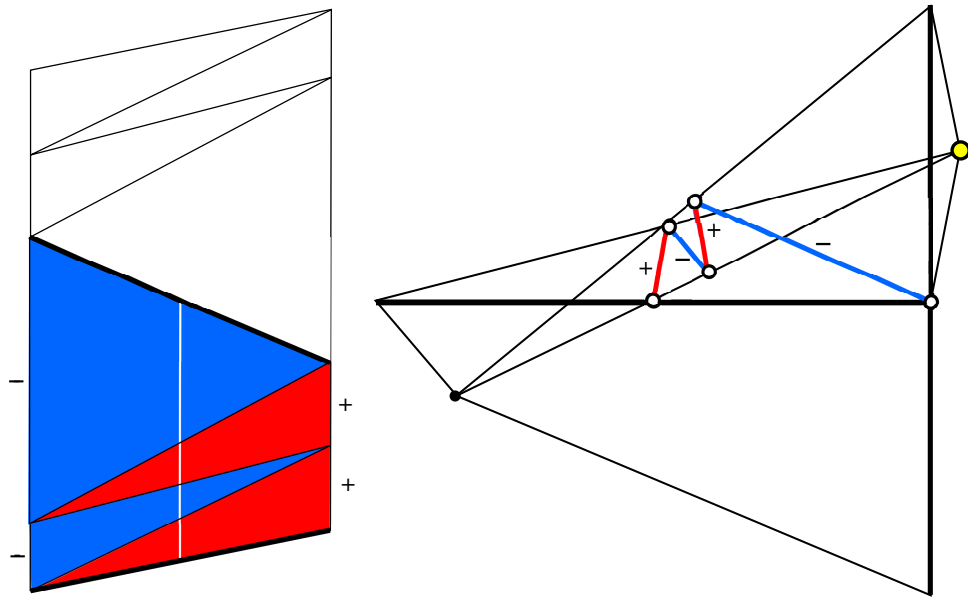


Figure 2.1: The bend pattern and the bottom half of the image

The Ridge Curve: We show the picture first, then explain.

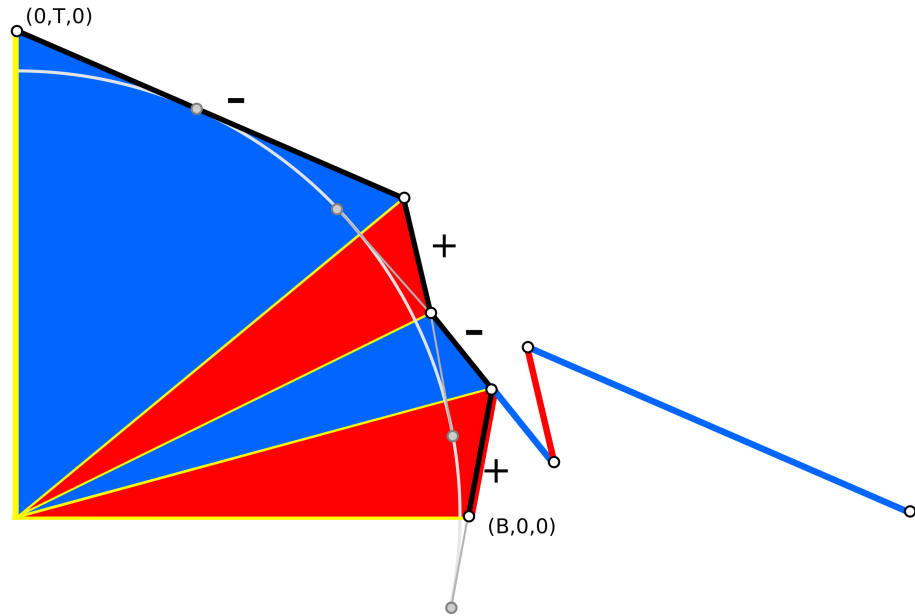


Figure 2.2: Half 2x core curve (red/blue) and half ridge curve (black).

Let β_b be the bottom edge of the parallelogram representing M_λ . We normalize so that I maps the left vertex of β_b to $(0, 0, 0)$ and the right vertex to $(B, 0, 0)$, where B is the length of β_b . Let E_1, \dots, E_n be the successive edges of the core curve, treated as vectors. Let

$$\Gamma'_i = 2\mu_i E_i, \quad i = 1, \dots, n. \quad (4)$$

Let Γ be the curve whose initial vertex is $(B, 0, 0)$ and whose edges are $\Gamma'_1, \dots, \Gamma'_n$. Here μ_1, \dots, μ_n is the sign sequence.

Γ has length 2λ , connects $(B, 0, 0)$ to $(-B, 0, 0)$, and is disjoint from the open unit ball. The lines extending the sides of Γ are tangent to the unit sphere. We rotate so that Γ contains $(0, T, 0)$ for some $T > 1$. If we cone Γ to the origin, we get a collection $\Delta_1, \dots, \Delta_n$ of triangles, and Δ_i is the translate of $\mu_i I(\delta_i)$ whose apex is at the origin. In particular, the vectors pointing to the vertices of Γ are parallel to the corresponding bend images. Figure 2.2 shows the portion of the ridge curve (in black) associated to the example in Figure 2.1. We have also scaled the core curve by 2 and translated it to show the relationships between the two curves.

2.2 Geometric Bounds

While we are in the neighborhood, we re-prove the lower bound from [FT]. The proof in [FT] is somewhat similar, though it does not use the ridge curve. Let λ be the aspect of the polygonal Moebius band \mathcal{M} and let Γ be the associated ridge curve. Let $f : \mathbf{R}^3 - B^3 \rightarrow S^2$ be orthogonal projection. The map f is arc-length decreasing. Letting $\Gamma^* = f(\Gamma)$, we have $|\Gamma^*| < |\Gamma| = 2\lambda$. Since Γ^* connects a point on S^2 to its antipode, $|\Gamma^*| \geq \pi$. Hence $\lambda > \pi/2$.

Now we use the same idea in a different way.

Lemma 2.1 *Suppose \mathcal{M} has aspect ratio less than $7\pi/12$. Then the ridge curve Γ lies in the open slab bounded by the planes $Z = \pm 1/\sqrt{2}$.*

Proof: We divide Γ into halves. One half goes from $(B, 0, 0)$ to $(0, T, 0)$ and the second half goes from $(0, T, 0)$ to $(-B, 0, 0)$. Call the first half Γ_1 . Suppose that Γ_1 intersects the plane $Z = 1/\sqrt{2}$. Then the spherical projection Γ_1^* goes from $A = (1, 0, 0)$ to some unit vector $B = (u, v, 1/\sqrt{2})$ to $C = (0, 1, 0)$. Here $u^2 + v^2 = 1/2$. The shortest path like this is the geodesic bigon connecting A to B to C . Such a bigon has length at least

$$\arccos(A \cdot B) + \arccos(B \cdot C) = \arccos(u) + \arccos(v) \geq^* 2 \arccos(1/2) = 2\pi/3.$$

The starred inequality comes from the fact that the minimum, subject to the constraint $u^2 + v^2 = 1/2$, occurs at $u = v = 1/2$.

But then Γ has length at least $2\pi/3 + \pi/2 = 7\pi/6$. This exceeds twice the aspect ratio of \mathcal{M} . This is a contradiction. The same argument works if Γ_1 hits the plane $Z = -1/\sqrt{2}$. Likewise the same argument works with the second half of Γ in place of the first half. ♠

Corollary 2.2 *Suppose \mathcal{M} has aspect ratio less than $7\pi/12$. Let β_1^* and β_2^* be two perpendicular bend images. Then a plane parallel to both β_1^* and β_2^* cannot contain a vertical line.*

Proof: Every bend image is parallel to some vector from the origin to a point of Γ . By the previous result, such a vector make an angle of less than $\pi/4$ with the XY -plane. Hence, all bend images make angles of less than $\pi/4$ with the XY -plane. Suppose our claim is false. Since β_1^* and β_2^* are perpendicular to each other, one of them must make an angle of at least $\pi/4$ with the XY -plane. This is a contradiction. ♠

2.3 Perpendicular Lines

As a prelude to the work in the next section, we prove a few results about lines and planes. Say that an *anchored line* in \mathbf{R}^3 is a line through the origin. Let Π_1 and Π_2 be planes through the origin in \mathbf{R}^3 .

Lemma 2.3 *Suppose that Π_1 and Π_2 are not perpendicular. The set of perpendicular anchored lines (L_1, L_2) with $L_j \in P_j$ for $j = 1, 2$ is diffeomorphic to a circle.*

Proof: For each anchored line $L_1 \in \Pi_1$ the line $L_2 = L_1^\perp \cap \Pi_2$ is the unique choice anchored line in Π_2 which is perpendicular to L_1 . The line L_2 is a smooth function of L_1 . So, the map $(L_1, L_2) \rightarrow L_1$ gives a diffeomorphism between the space of interest to us and a circle. ♠

A *sector* of the plane Π_j is a set linearly equivalent to the union of the $(++)$ and $(--)$ quadrants in \mathbf{R}^2 . Let $\Sigma_j \subset \Pi_j$ be a sector. The boundary $\partial\Sigma_j$ is a union of two anchored lines.

Lemma 2.4 *Suppose (again) that the planes Π_1 and Π_2 are not perpendicular. Suppose also that no line of $\partial\Sigma_1$ is perpendicular to a line of $\partial\Sigma_2$. Then the set of perpendicular pairs of anchored lines (L_1, L_2) with $L_j \in \Sigma_j$ for $j = 1, 2$ is either empty or diffeomorphic to a closed line segment.*

Proof: Let S^1 denote the set of perpendicular pairs as in Lemma 2.3. Let $X \subset S^1$ denote the set of those pairs with $L_j \in \Sigma_j$. Let π_1 and π_2 be the two diffeomorphisms from Lemma 2.3. The set of anchored lines in Σ_j is a line segment and hence so is its inverse image $X_j \subset S^1$ under π_j . We have $X = X_1 \cap X_2$. Suppose X is nonempty. Then some $p \in X$ corresponds to a pair of lines (L_1, L_2) with at most one $L_j \in \partial\Sigma_j$. But then we can perturb p slightly, in at least one direction, so that the corresponding pair of lines remains in $\Sigma_1 \times \Sigma_2$. This shows that $X_1 \cap X_2$, if nonempty, contains more than one point. But then the only possibility, given that both X_1 and X_2 are segments, is that their intersection is also a segment. ♠

2.4 The Space of Perpendicular Pairs

We prove the results in this section more generally for piecewise affine maps $I : M_\lambda \rightarrow \mathbf{R}^3$ which are not necessarily local isometries. The reason for the added generality is that it is easier to make perturbations within this category. Let \mathbf{X} be the space of such maps which also satisfy the conclusion of Corollary 2.2. (In this section we will not use this property but in the next section we will.) So, \mathbf{X} includes all (isometric) polygonal Moebius bands of aspect ratio less than $7\pi/12$. The notions of bend images and facets makes sense for members of \mathbf{X} .

Lemma 2.5 *The space \mathbf{X} has a dense set \mathbf{Y} which consists of members such that no two facets lie in perpendicular planes and no two special bend images are perpendicular.*

Proof: One can start with any member of \mathbf{X} and postcompose the whole map with a linear transformation arbitrarily close to the identity so as to get a member of \mathbf{Y} . The point is that we just need to destroy finitely many perpendicularity relations. ♠

Let γ be center circle of M_λ . We can identify the space of bend images of \mathcal{M} with γ : The bends and bend-images are in bijection, and each bend intersects γ once. The space of ordered pairs of unequal bend images can be identified with $\gamma \times \gamma$ minus the diagonal. We compactify this space by adding in 2 boundary components. One of the boundary components comes from approaching the main diagonal from one side and the other comes from approaching the diagonal from the other side. The resulting space A is an annulus. For the rest of the section we choose a member of \mathbf{Y} and make all definitions for this member.

Lemma 2.6 \mathcal{P} is a piecewise smooth 1-manifold in A .

Proof: We apply Lemma 2.4 to the planes through the origin parallel to the facets and to the anchored lines parallel to the bend images within the facets. (Within a single facet the bend images and the corresponding anchored lines are in smooth bijection.) By Lemma 2.4, the space \mathcal{P} is the union of finitely many smooth connected arcs. Each arc corresponds to an ordered pair of facets which contains at least one point of \mathcal{P} . Each of these arcs has two endpoints. Each endpoint has the form (β_1^*, β_2^*) where exactly one of these bend images is special. Let us say that β_1^* is special. Then β_1^* is the edge between two consecutive facets, and hence (β_1^*, β_2^*) is the endpoint of exactly 2 of the arcs. Hence the arcs fit together to make a piecewise smooth 1-manifold. ♠

A component of \mathcal{P} is *essential* if it separates the boundary components of A .

Lemma 2.7 \mathcal{P} has an odd number of essential components.

Proof: An essential component, being embedded, must represent a generator for the first homology $H_1(A) = \mathbf{Z}$. By duality, a transverse arc running from one boundary component of A to the other intersects an essential component an odd number of times and an inessential component an even number of times. Let a be such an arc. As we move along a the angle between the corresponding bends can be chosen continuously so that it starts at 0 and ends at π . Therefore, a intersects \mathcal{P} an odd number of times. But this means that there must be an odd number of essential components of \mathcal{P} . ♠

2.5 The Main Argument

Now we prove Lemma 1.2. Say that a member of \mathbf{X} is *good* if (with respect to this member) there is a path connected subset $\mathcal{K} \subset \mathcal{P}$ such that both (β_1^*, β_2^*) and (β_2^*, β_1^*) belong to \mathcal{K} for some pair (β_1^*, β_2^*) .

Lemma 2.8 *If \mathcal{M} is good then \mathcal{M} has a T -pattern.*

Proof: Each pair (β_1^*, β_2^*) in \mathcal{P} determines a unique pair of parallel planes (P_1, P_2) such that $\beta_j^* \subset P_j$ for $j = 1, 2$. By hypothesis, members These planes do not contain vertical lines. Hence, our planes intersect the Z -axis in single and continuously varying points. As we move along \mathcal{K} these planes exchange places and so do their Z -intercepts. So, at some instant, the planes coincide and give us a T -pattern. ♠

Lemma 2.9 *A dense set of members of \mathbf{X} are good.*

Proof: Let \mathbf{Y} be the dense subset of \mathbf{X} considered in the previous section. Relative to any member of \mathbf{Y} , the space \mathcal{P} is a piecewise smooth 1-manifold of the annulus A with an odd number of essential components. The involution ι , given by $\iota(p_1, p_2) = (p_2, p_1)$, is a continuous involution of A which preserves \mathcal{P} and permutes the essential components. Since there are an odd number of these, ι preserves some essential component of \mathcal{P} . But then this essential component contains our set \mathcal{K} . ♠

Now we know that there are T -patterns for members of a dense subset of \mathbf{X} . By compactness and continuity, every member of \mathbf{X} has a T -pattern. By Corollary 2.2, \mathbf{X} contains all (ordinary) embedded polygonal Moebius bands of aspect ratio less than $7\pi/12$. Hence all such embedded Moebius bands contain T -patterns. This completes the proof of Lemma 1.2.

3 The Aspect Ratio Bound

3.1 Constraints coming from the T Pattern

Let \mathcal{M} be a polygonal Moebius band of aspect ratio $\lambda < 7\pi/12$. We keep the notation from the previous chapter.

Let β_1 and β_2 be two bends whose corresponding images $\beta_1^* = I(\beta_1)$ and $\beta_2^* = I(\beta_2)$ form a T -pattern. Since these segments do not intersect, we can label so that the line extending β_2^* does not intersect β_1^* . We cut M_λ open along β_1 and treat β_1 as the bottom edge. We now set $\beta_b = \beta_1$ and $\beta_t = \beta_2$ and (re)normalize as in §2.1. So, β_b^* connects $(0, 0, 0)$ to $(B, 0, 0)$, and β_t^* is a translate of the segment connecting $(0, 0, 0)$ to $(0, T, 0)$. Here B and T are the lengths of these segments.

The left side of Figure 3.1 shows M_λ . Reflecting in a vertical line, we normalize so that $L_1 \geq R_1$. This means that $L_2 \geq R_2$. The right side of Figure 3.1 shows that T pattern, and the corresponding images of the sets on the left under the isometry I . The wiggly curves we have drawn do not necessarily lie in the XY -plane but their endpoints do.

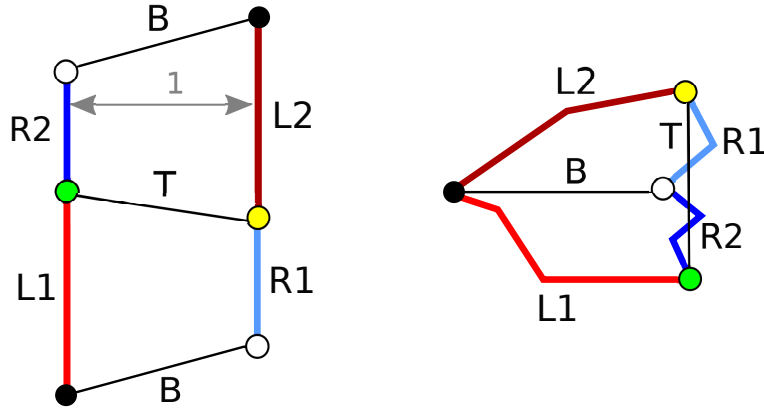


Figure 3.1: A Paper Moebius band interacting with the T -pattern.

There is some ϵ such that the vertical distance (i.e., the difference in the y -coordinates) from the white vertex to the yellow vertex is $T/2 + \epsilon$ and the vertical distance from the white vertex to the green vertex is $T/2 - \epsilon$.

Looking at the picture, and using the fact that geodesics in the Euclidean plane are straight lines, we get the following constraints:

$$R_1 + R_1 \geq T, \quad (5)$$

$$L_1 + L_2 \geq \sqrt{B^2 + (T/2 - \epsilon)^2} + \sqrt{B^2 + (T/2 + \epsilon)^2} \geq 2\sqrt{B^2 + T^2/4}. \quad (6)$$

3.2 An Optimization Problem

We are done with the Moebius band. We just have a parallelogram as on the left side of Figure 3.1 which satisfies the constraints in Equations 5 and 6 and we want to minimize $L_1 + L_2 + R_1 + R_2$. Let $L = (L_1 + L_2)/2$ and $R = (R_1 + R_2)/2$. If we replace L_1, L_2 by L, L and R_1, R_2 by R, R the constraints are still satisfied and the sum of interest is unchanged. The constraints now become:

$$2R \geq T, \quad L \geq \sqrt{B^2 + T^2/4}. \quad (7)$$

We show that $L + R \geq \lambda_1$, the constant from the Main Theorem, which means

$$\lambda = \frac{1}{2}(L_1 + L_2 + R_1 + R_2) = L + R \geq \lambda_1.$$

So, showing that $L + R \geq \lambda_1$ finishes the proof of the Main Theorem.

Let b and t respectively denote the slopes of the sides labeled B and T in Figure 3.2. Let $S = L + R$. Since $L \geq R$ we have $b \geq t$. In Figure 3.2 we depict the case when $b > 0$ and $t < 0$. We mention without proof that this must happen when $S < \sqrt{3}$. (Our sequel paper has a proof.)

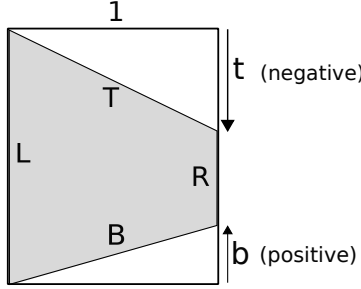


Figure 3.2: The basic trapezoid.

Since $L + R = S$ and $L - R = b - t$, and by the Pythagorean Theorem,

$$L = \frac{S + b - t}{2}, \quad R = \frac{S - b + t}{2}, \quad B = \sqrt{1 + b^2}, \quad T = \sqrt{1 + t^2}. \quad (8)$$

Plugging these relations into Equation 7, we get $S \geq f(b, t)$ and $S \geq g(b, t)$ where

$$f(b, t) = b - t + T, \quad g(b, t) = -b + t + \sqrt{4B^2 + T^2}.$$

Let $\phi = \max(f, g)$ and let D be the domain where $b \geq t$. We have $S \geq \phi$. To finish the proof of the Main Theorem we just need to show that $\min_D \phi = \lambda_1$. This is what we do.

Lemma 3.1 ϕ achieves its minimum at a point in the interior of D , and at this point we have $f = g$.

Proof: We note 3 properties of our functions:

1. $f(0, -1/\sqrt{3}) = g(0, -1/\sqrt{3}) = \sqrt{3}$. Hence $\phi(0, -1/\sqrt{3}) = \sqrt{3}$.
2. On ∂D we have $g(b, b) = B\sqrt{5} \geq \sqrt{5}$. Hence $\min_{\partial D} \phi > \sqrt{3}$.
3. As $b^2 + t^2 \rightarrow \infty$ in D , we have $f, g \rightarrow +\infty$.

From these properties, we see that the global minimum of ϕ is achieved at some point in the interior of D . Next, we compute

$$\frac{\partial f}{\partial t} = -1 + \frac{t}{T} < 0, \quad \frac{\partial g}{\partial t} = 1 + \frac{t}{4B^2 + T^2} > 0.$$

Hence the gradients of f and g are never zero, and are never positive multiples of each other. For this reason, any point where ϕ achieves a global minimum lies on the set where $f = g$. ♠

Setting $f = g$ and solving for b , we get

$$b = \beta(t) = \frac{t^3 - T^3 - 3t}{3t^2 - 1}. \quad (9)$$

There no solutions to $f = g$ when $t = +1/\sqrt{3}$ and Item 1 above (or a direct calculation) shows that $\beta(-1/\sqrt{3}) = 0$. In particular, β has a removable singularity at $t = -1/\sqrt{3}$ and hence is smooth on the domain

$$D^* = (-\infty, 1/\sqrt{3}).$$

When $t > 1/\sqrt{3}$ we have $b = \beta(t) < 0 < t$. Hence, only $t \in D^*$ corresponds to points in D . So, we just need show $\min_{D^*} \phi^* = \lambda_1$, where

$$\phi^*(t) = f(\beta(t), t) = \frac{2T(t^2 - tT - 1)}{3t^2 - 1} \quad (10)$$

As $t \rightarrow -\infty$ or $t \rightarrow 1/\sqrt{3}$ we have $\phi^*(t) \rightarrow +\infty$. Hence ϕ^* achieves its minimum on D^* at some point where $d\phi^*/dt = 0$. This happens only at

$$t_0 = -\sqrt{\frac{2}{\sqrt{3}} - 1} = -.39332\dots$$

We check that $\phi^*(t_0) = \lambda_1$.

4 Polygonal Approximation

In this short chapter we explain why the results in the polygonal case imply the results in the smooth case. There is some subtlety here because the obvious method of polygonal approximation (described below) does not quite yield the polygonal Moebius bands that we have been working with. We need to broaden the definition.

A K -bilipschitz map between metric spaces is one which distorts distances by a factor of at most K . A 1-bilipschitz map is an isometry. Say that a K -bilipschitz polygonal Moebius band is the same kind of map as a polygonal Moebius band, except that the restriction of the map to each triangle is linear and K -bilipschitz. All the arguments in this paper work the same way for K -bilipschitz polygonal Moebius bands as they do for 1-bilipschitz polygonal Moebius bands, except that the bound $\lambda > \lambda_1$ in the Main Theorem is replaced by $\lambda > \lambda_1/K$. Lemma 1.2 has a similar easy modification.

The following result justifies the claim that “polygonal implies smooth”,

Lemma 4.1 *Let $I' : M_\lambda \rightarrow \mathbf{R}^3$ be a smooth paper Moebius band. There is a sequence of K_n -bilipschitz polygonal Moebius bands $I_n : M_\lambda \rightarrow \mathbf{R}^3$ with $K_n \rightarrow 1$, so that:*

1. *For each $p \in M_\lambda$ we have $\|I'(p) - I_n(p)\| < K_n - 1$.*
2. *If I_n is linear about p then the plane tangent to $I_n(M_\lambda)$ at $I_n(p)$ makes an angle less than $K_n - 1$ with the tangent plane to $I'(M_\lambda)$ at $I'(p)$.*

I_n is an embedding for n large provided that I' is an embedding.

Proof: We take a large finite mesh β_0, \dots, β_n of bends in M_λ , with β_0 being the first bend and β_n being the last. The union

$$\partial M_\lambda \cup \beta_0 \cup \dots \cup \beta_n$$

is a union of n trapezoids, some possibly degenerate – i.e. triangles. For each nondegenerate trapezid we insert one of the two diagonals. This gives us a triangulation of M_λ of the kind considered above. The restriction of I' to $\beta_0 \cup \dots \cup \beta_n$ gives us exactly enough information to extend linearly to all of M_λ by making the map linear on each triangle of the triangulation. Call the resulting map I_n .

Given the compactness of M_λ and the smoothness of I' , the map I_n is a K_n -bilipschitz polygonal Moebius band with $K_n \rightarrow 1$. Because I' and I_n agree on a set which is becoming dense in M_λ as $n \rightarrow \infty$, these maps satisfy Condition 1 above. Now we justify Condition 2. Given the regularity of I' , the convex hull of the images $I(\beta_j)$ and $I(\beta_{j+1})$ will be nearly flat, in the sense that the 4 faces of this tetrahedron will be all nearly parallel to each other, and all faces be nearly parallel to the tangent planes to $I'(M_\lambda)$ at nearby points.

The final statement about the embedding follows from the C^1 nature of the approximation. ♠

5 References

[AHLM] A. Malaga, S. Lelievre, E. Harriss, P. Arnoux,
ICERM website: <https://im.icerm.brown.edu/portfolio/paper-flat-tori/> (2019)

[CF] Y. Chen and E. Fried, *Möbius bands, unstretchable material sheets and developable surfaces*, Proceedings of the Royal Society A, (2016)

[CKS] J. Cantarella, R. Kusner, J. Sullivan, *On the minimum ropelength of knots and links*, Invent. Math. **150** (2) pp 257-286 (2003)

[FT], D. Fuchs, S. Tabachnikov, *Mathematical Omnibus: Thirty Lectures on Classic Mathematics*, AMS 2007

[HF], D.F. Hinz, E. Fried, *Translation of Michael Sadowsky's paper 'An elementary proof for the existence of a developable Möbius band and the attribution of the geometric problem to a variational problem'*. J. Elast. 119, 3–6 (2015)

[HW], B. Halpern and C. Weaver, *Inverting a cylinder through isometric immersions and embeddings*, Trans. Am. Math. Soc **230**, pp 41.70 (1977)

[MK] L. Mahadevan and J. B. Keller, *The shape of a Möbius band*, Proceedings of the Royal Society A (1993)

[Sa], M. Sadowski, *Ein elementarer Beweis für die Existenz eines abwickelbaren Möbiuschen Bandes und die Zurückführung des geometrischen Problems auf ein Variationsproblem*. Sitzungsberichte der Preussischen Akad. der Wissenschaften, physikalisch-mathematische Klasse 22, 412–415.2 (1930)

[S1] G. Schwarz, *A pretender to the title “canonical Moebius strip”*, Pacific J. of Math., **143** (1) pp. 195-200, (1990)

[S2] R. E. Schwartz, *The 5 Electron Case of Thomson's Problem*, Journal of Experimental Math, 2013.

[W] S. Wolfram, *The Mathematica Book, 4th Edition*, Wolfram Media and Cambridge University Press (1999).